Proceedings of the ASME 2010 3rd Joint US-European Fluids Engineering Summer Meeting and 8th International Conference on Nanochannels, Microchannels, and Minichannels
FEDSM-ICNMM2010
August 1-5, 2010, Montreal, Canada

FEDSM-ICNMM2010-30832

LOCAL THERMAL EQUILIBRIUM IN FORCED CONVECTION THROUGH POROUS MEDIA

A. Nouri-Borujerdi
Department of Mechanical Engineering
Islamic Azad University, South Tehran Branch, Tehran, IRAN

ABSTRACT

Forced convection heat transfer through a channel filled with a porous medium is investigated using perturbation method. Two-energy equation model is utilized to represent the assumption of local thermal non-equilibrium which exists between the solid and fluid phases. The Brinkman-Forchheimer extension of the Darcy model is used to represent the fluid transport within the porous medium. Analytical solution is obtained for both fluid and solid temperature fields incorporating the effects of various pertinent parameters such as the Darcy number, the Biot number, the thermal conductivity and the pressure gradient. It is found that the Darcy number and the pressure gradient have significant effects on the local thermal equilibrium assumption.

NOMENCLATURE

a	Interfacial area per unit volume
Bi	Biot number
Da	Darcy number
F	function
h	Heat transfer coefficient
H	one half of channel height
K	permeability
k	Thermal conductivity
P	pressure
$\dot{q}''$	Heat flux
T	temperature
u	axial velocity
x	x- coordinate
y	y- coordinate

Greek letters

ε	porosity
Λ	Inertia parameter
μ	viscosity
ν	Kinematics viscosity
θ	Non-dimensional temperature
ρ	density

Subscripts

sf	Solid fluid
f	fluid
s	solid
w	wall
eff	effective

Superscripts

f	fluid
s	solid
*	Non-dimensional

INTRODUCTION

Forced convective heat transfer in porous media has been the subject of many recent studies due to numerous practical applications such as thermal insulation, packed bed heat exchangers, heat pipes, electronic cooling, drying technology, catalytic reactors, nuclear waste repository, energy storage units, petroleum technology and geothermal systems. The assumption of local thermal equilibrium is widely used in many of these applications .However, this assumption breaks down when a substantial temperature difference exists between the solid and fluid phases. More recently local thermal non-equilibrium has received considerable attention due to its pertinence in applications where such a differential exists between the solid and the fluid phases.

Koh and Colony [1] used quite a restricted two-equation model which did not account for various important effects such as conduction through the fluid phase, dispersion and non-Darcian effects. Vafai and Sozen [2] investigated forced convective flow through porous media utilizing a rigorous formulation based on locally volume average two–equation model. They provided detailed insight relative to momentum transport and thermal characteristics within porous media. Later on Amiri and Vafai [3, 4] employed a general fluid flow model and a two-phase energy equation to investigate the forced convective heat transfer within the channel with constant wall temperature. They included the effect of variable porosity and thermal dispersion in their analysis and error maps for assessing the importance of various simplifying assumptions that are commonly used were established their

work. Some additional aspects of the local thermal equilibrium have been presented by Whitaker [5] and Sozen and Vafai[6]. The work of Vafai and Tien [7] was one of the early attempts to account for the boundary and inertia effects in the momentum equation for a porous media. They found that the momentum boundary layer thickness is of the order of $\sqrt{K/\varepsilon}$. Vafai and Thiyagaraj [8] presented analytical solution for the velocity and temperature fields of the interface region using the Brinkman–Forchheimer extended Darcy equation. They considered three fundamental types of the interface namely, the interface between two porous media, the interface between a porous medium and a fluid layer and the interface between a porous medium and an impermeable medium. Lee and Vafai [9] employed the non thermal equilibrium model to investigate the forced convective flow through a channel filled with the porous medium subject to a constant heat flux. They obtained analytical solution for the fluid and solid phase temperature distributions. In their work, validity of one–equation model was presented considering a Darcian fluid flow. Kim et al. [10] presented an analytical solution for the two–equation model including the boundary effects for an equivalent micro channel application. They presented analytical solution for the fluid and solid phase temperature distribution based on the Brinkman-extended Darcy equation. They also analyzed the validity of the local thermal equilibrium assumption.

In this work, the Brinkman–Forchheimer extended Darcy model is used to obtain an analytical solution for the fluid and solid phase temperature distributions in a channel under a constant wall heat flux. The two-equation model is used because of the local thermal non-equilibrium assumption. Errors characterizing validity of the thermal equilibrium are obtained for a range of Darcy and inertia numbers as well as non–Darcy effects on temperature differentials in porous media are established.

Modeling and Formulation

Consider a fully developed flow in a plane duct filled with a porous medium subjected to a constant wall heat flux, (Fig.1). Due to the symmetrical flow about the center line, one half of the channel is considered. The momentum equation accounting for the inertia and boundary effects is:

$$\frac{\mu}{\varepsilon}\frac{\partial^2 u}{\partial y^2}-\frac{\mu}{K}u-\frac{\varepsilon F}{\sqrt{K}}\rho_f |u|u-\frac{\partial P}{\partial x}=0 \tag{1}$$

The energy equations of the solid and fluid phases under non-thermal equilibrium condition are respectively as follows.

$$(k_s)_{eff}\frac{\partial^2 T_S}{\partial y^2}-a\,h_{sf}\,(T_S-T_f)=0 \tag{2}$$

$$(k_f)_{eff}\frac{\partial^2 T_f}{\partial y^2}+a\,h_{sf}\,(T_S-T_f)=\rho_f u C_{Pf}\frac{\partial T_f}{\partial x} \tag{3}$$

where u and T have been defined based on the local volume average velocity. $(k_S)_{eff}=(1-\varepsilon)k_S$ and $(k_f)_{eff}=\varepsilon k_f$

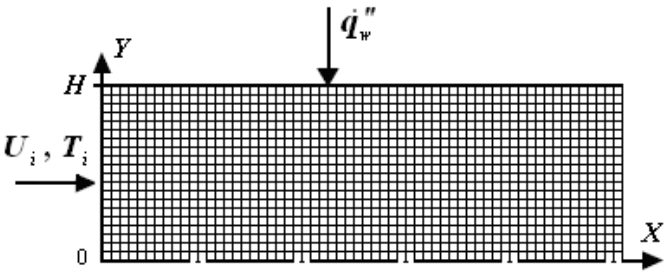

Fig.1. Schematic of one half of a parallel-plate duct filled with porous medium

Boundary Conditions: The fluid boundary conditions for velocity and temperature fields are represented by:

$$\frac{\partial u(0)}{\partial y}=0,\qquad u(H)=0 \tag{4}$$

$$T_f(H)=T_s(H) \tag{5}$$

$$\frac{\partial T_f(0)}{\partial y}=\frac{\partial T_s(0)}{\partial y}=0 \tag{6}$$

$$q_w=(k_f)_{eff}\frac{\partial T_f(H)}{\partial y}+(k_s)_{eff}\frac{\partial T_s(H)}{\partial y} \tag{7}$$

If the following dimensionless variables are introduced,

$$x^*=\frac{x}{H},\qquad y^*=\frac{y}{H},\qquad u^*=\frac{u}{u_i},\qquad Da=\frac{K}{H^2}$$

$$Bi=\frac{a\,h_{sf}H^2}{(k_s)_{eff}},\qquad k^*=\frac{(k_f)_{eff}}{(k_s)_{eff}}\qquad P^*=\frac{P}{\mu u_i/H}$$

$$Re_H=\frac{Hu_i}{\nu},\qquad \Lambda=\frac{F\,\mathrm{Re}_H}{\sqrt{Da}},\qquad \theta=\frac{T-T_w}{H\dot{q}''_w/(k_s)_{eff}}$$

the dimensional Eqs. (1-7) are respectively.

$$\frac{\partial^2 u^*}{\partial y^{*2}}-\frac{\varepsilon}{Da}u^*-\Lambda\varepsilon^2 u^{*2}-\varepsilon\frac{dP^*}{dx^*}=0 \tag{8}$$

$$k^*\frac{\partial^2\theta_f}{\partial y^{*2}}+Bi\,(\theta_s-\theta_f)=u^* \tag{9}$$

$$\frac{\partial^2\theta_s}{\partial y^{*2}}-Bi\,(\theta_s-\theta_f)=0 \tag{10}$$

The above equation is obtained by using the fully developed condition and $\rho_f c_p u_i \, \partial T_f / \partial x = \dot{q}''_w / H$ for a control volume in Fig. (1). T_f is the local volume average.

$$\frac{\partial u^*(0)}{\partial y^*} = 0, \quad u^*(1) = 0 \tag{11}$$

$$\theta_f(1) = 0, \quad \theta_s(1) = 0 \tag{12a-b}$$

$$\frac{\partial \theta_f(0)}{\partial y^*} = 0, \quad \frac{\partial \theta_s(0)}{\partial y^*} 0 \tag{13a-b}$$

$$k^* \frac{\partial \theta_f(1)}{\partial y^*} + \frac{\partial \theta_s(1)}{\partial y^*} = 1 \tag{14}$$

ANALYSIS

Velocity profile: Assuming dP^*/dx^* = constant in Eq. (8) and **i**nvoking the singular perturbation method, we can find the velocity profile as.

$$u^* = u_0^* + \varepsilon u_1^* + \varepsilon^2 u_2^* \tag{15}$$

Utilizing Eq. (11), the velocity profile will be read as:

$$u^* = -\frac{dP^*}{dx^*}\left[\frac{\varepsilon}{2}\left(1 - y^{*2}\right) + \varepsilon^2 \frac{y^{*4} - 6y^{*2} + 5}{24Da}\right] \tag{16}$$

Appling the mass balance across the channel, one can simply obtain $-dp^*/dx^* = 15Da/\varepsilon(5Da + 2\varepsilon)$. Substituting the result into Eq. (16), the final result is:

$$u^* = \frac{5(12Da + 5\varepsilon)}{8(5Da + 2\varepsilon)} - \frac{15(2Da + \varepsilon)}{4(5Da + 2\varepsilon)} y^{*2} + \frac{5\varepsilon}{8(5Da + 2\varepsilon)} y^{*4} \tag{17}$$

Temperature profile: Combining the two coupled energy Eqs. Eqs. (9) and (10), the fluid differential equation will be.

$$k^* \frac{d^4\theta_f}{dy^{*4}} - Bi(1 + k^*)\frac{d^2\theta_f}{dy^{*2}} = -Biu^* + \frac{d^2u^*}{dy^{*2}} \tag{18}$$

The solution of the above equation is sum of a particular integral of the non-homogeneous and complementary function of the corresponding homogeneous equation. After introducing Eq. (17), the result is as follows.

$$\theta_f = -\left[\frac{A}{2\lambda^2} + \frac{B}{\lambda^4} + \frac{12C}{\lambda^6}\right] y^{*2} - \left[\frac{B}{12\lambda^2} + \frac{C}{\lambda^4}\right] y^{*4} - \frac{C}{30\lambda^2} y^{*6} + a_o + a_1 y^* + a_2 e^{\lambda y^*} + a_3 e^{-\lambda y^*} \tag{19}$$

where $\lambda = \sqrt{\beta i\left(1 + 1/k^*\right)}$

Two more sets of boundary conditions are required to solve the above fourth–order differential equations. These are obtained by applying the boundary conditions given by Eqs. (12) and (13) to Eq. (9).

$$\theta_f''(1) = 0 \tag{20}$$

$$\theta_f'''(0) = 0 \tag{21}$$

Applying the boundary conditions given by Eqs. (21), (13a) and (12a), after a lengthy process we have:

$$a_2 = a_3 \tag{22}$$

$$a_1 = 0 \tag{23}$$

$$a_2 = \left[\begin{array}{l} \beta i + (1-\varepsilon)\dfrac{15Da + 5\varepsilon}{5Da + 2\varepsilon} + \beta i \dfrac{15A + 5B + 3C}{15\lambda^2} + \\ \left[\varepsilon\beta i k^* + (1-\varepsilon)(1-k^*)\right]\left[\dfrac{24C}{\lambda^6} + \dfrac{2B + 4C}{\lambda^4}\right] \end{array}\right] \times \left[(4\varepsilon - 2)\lambda\beta i k^* \sinh\lambda\right]^{-1} \tag{24}$$

Introducing the fluid temperature into Eq. (9), the solid temperature reads.

$$\theta_s = \theta_f - \frac{k^*}{\beta i}\frac{\partial^2\theta_f}{\partial y^{*2}} + \frac{u^*}{\beta i} \tag{25}$$

The temperature difference between the fluid and solid is obtained from:

$$\theta_s - \theta_f = \frac{k^*}{\beta i}\left[\begin{array}{l} \dfrac{24C}{\lambda^6} + \dfrac{2B}{\lambda^4} + \dfrac{A}{\lambda^2} + \left(\dfrac{B}{\lambda^2} + \dfrac{12C}{\lambda^4}\right) y^{*2} \\ + \dfrac{C}{\lambda^2} y^{*4} - 2a_2\lambda^2 \cosh y^* + \dfrac{u^*}{k^*} \end{array}\right] \tag{26}$$

RESULTS AND DISCUSSION

Fig. 2 shows the temperature profiles of the solid and fluid phases across the channel flow from the center line towards the wall for $dp^*/dx^* = 10^{-3}$, Da=10^{-4} and $k^*=10^{-3}$. Enhancement of the Biot number causes the solid phase temperature is close to the fluid temperature. In other words, the assumption of local thermal equilibrium exits between the two phases. As such, the temperature gradient at any location between the two phases is assumed to be negligible. On the other hand, when the Biot number is small, there is a big temperature difference between the two phases and the assumption of the local thermal equilibrium condition will break down. In addition, the local non-thermal equilibrium at the centre line of the porous channel is more prominent than the other locations. In this case, heat transfer between the two phases should be included.

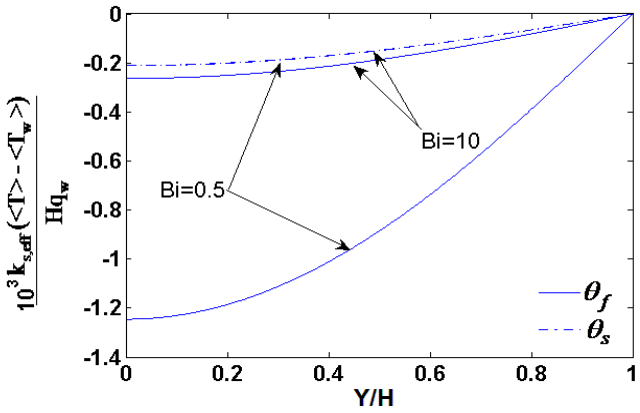

Fig. 2 Temperature distribution of the solid and fluid across the channel for $dp^*/dx^* = 10^{-3}$, Da=10^{-4} and $k^*=10^{-3}$

Fig. 3 illustrates the same temperature distribution trend as the previous one except for $k^*=0.1$. The scale of the temperature profiles on the ordinate axis is increased by two orders of magnitude in comparison with Fig. 2. The solid phase temperatures start to be separated from each other for $Bi = 0.5$ and 10 when $k^*=0.1$, whereas this case has not been occurred for $k^*=10^{-3}$. Because of employing the boundary conditions, the difference between these two doted lines is zero at the wall and is a maximum on the centre line.
Figs. 4 and 5 demonstrate the temperature difference profiles between the solid and fluid phases for $dp^*/dx^* = 0.5$, Da=10^{-4} and different values of the controlling parameters such as Biot number and the ratio of the effective fluid conductivity to that of the solid, k^*. The previous discussions are valid here too. As we can see, the trends of the profiles in Figs. 4 and 5 are similar to that of the Figs. 2 and 3. The scale of the temperature on the ordinate axis in Figs. 4 and 5 has been increased by three orders of magnitude relative to the Figs. 2 and 3. This is because of a large pressure gradient along the channel flow. As a result of increasing the pressure gradient, the mass flow rate increases too and causes the temperature difference rises. Again, the temperature of the solid phase starts to be separated from each other for $Bi = 0.5$ and 10 when $k^*=0.1$.

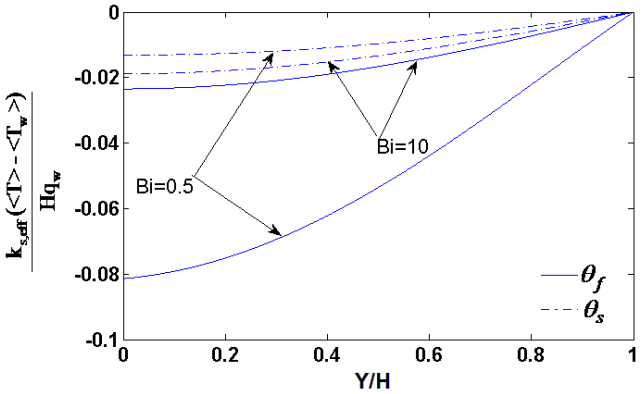

Fig. 3 Temperature distribution of the solid and fluid across the channel for $dp^*/dx^* = 10^{-3}$, Da=10^{-4} and $k^*=0.1$

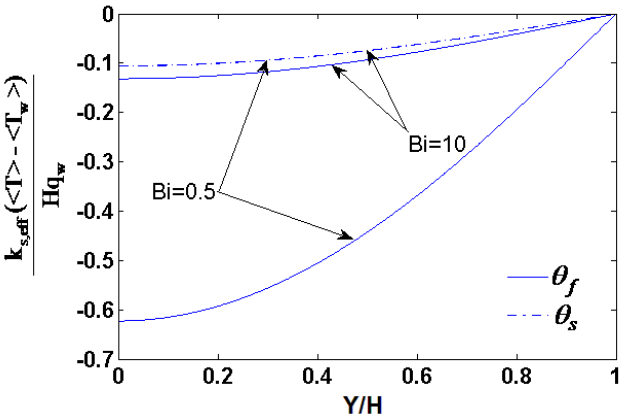

Fig. 4 Temperature distribution of the solid and fluid across the channel for $dp^*/dx^* = 0.5$, Da=10^{-4} and $k^*=10^{-3}$

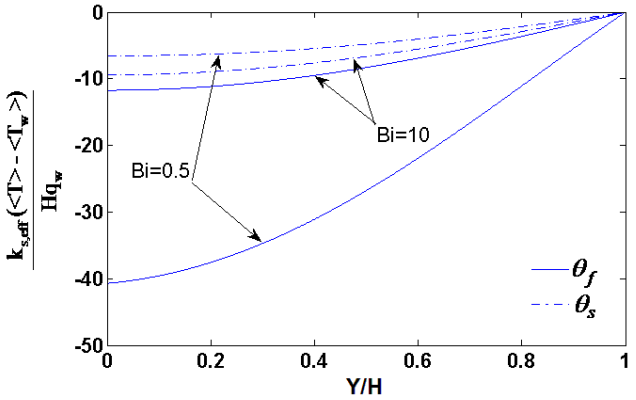

Fig. 5 Temperature distribution of the solid and fluid across the channel for $dp^*/dx^* = 0.5$, Da=10^{-4} and $k^*=0.1$

Figs. 6 and 7 report the effect of the pressure gradient on the temperature profiles. As it can be seen, the pressure gradient has an important role so that changing dp^*/dx^* from 0.001 to 0.5 causes the dimensionless fluid temperature jumps from -800 to -4×10^5 at the channel centre line.

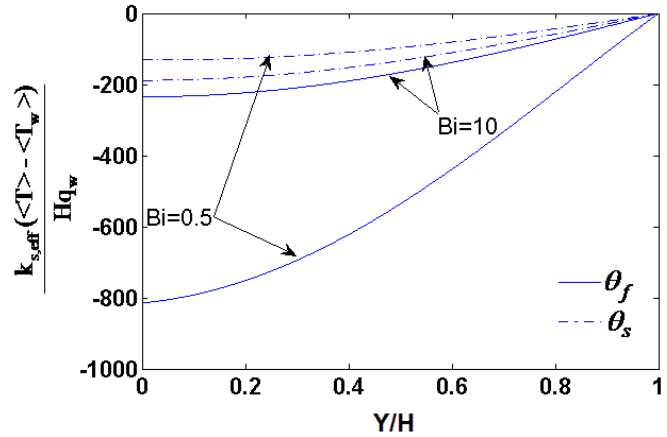

Fig.6, Temperature distribution of the solid and fluid phases across the channel, $dp^*/dx^* = 10^{-3}$, $Da = 10^{-8}$, $k^* = 0.1$

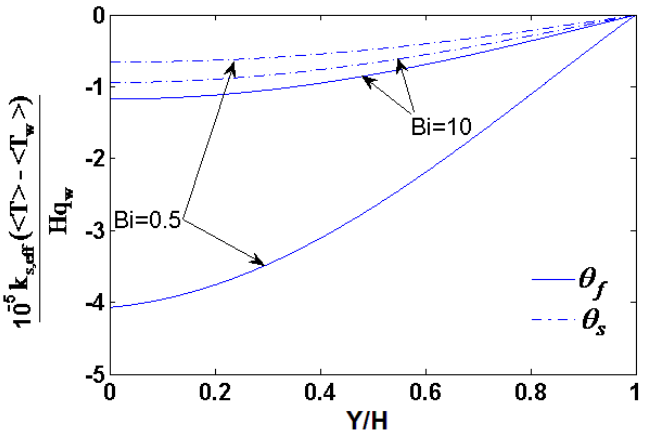

Fig. 7, Temperature distribution of the solid and fluid phases across the channel for $dp^*/dx^* = 0.5$, $Da = 10^{-8}$ and $k^* = 0.1$

CONCLUSIONS

Forced convective heat transfer through a channel filled with a porous medium was investigated analytically by the perturbation technique for the Brinkman Forchheimer extended Darcy model. The energy equations of the solid and fluid phases were used employing a non-thermal equilibrium model. The temperature field for both phases was obtained incorporating the effects of Biot number, Darcy number, pressure gradient and the conductivity ratio. The temperature difference between the two phases was found to decrease with an increase in the Biot number due to higher internal convection between the two phases. While an increase in the thermal conductivity ratio, k^*, resulted in a relative increase in fluid conduction throughout instead of being confined near the channel center. It was also established that the Darcy number and the Pressure gradient have a significant role on the local thermal equilibrium.

REFERENCES

[1] Koh, J.C.Y, .Colony, R, 1974, Analysis of cooling effectiveness for porous material in a coolant passage, *J. Heat Transfer*, 96, pp. 324-330.

[2] Vafai, K, Sozen, M, 1990, Analysis of energy and momentum transport for fluid flow through a porous bed, *J. Heat Transfer*, 112, pp.690-699.

[3] Amiri, A, Vafai, K, 1994, Analysis of dispersion effects and non thermal equilibrium, non Darcian, variable porosity incompressible flow through porous media, *Int. J. Heat Mass Transfer,* 37, pp.939-954.

[4] Amiri, A, Vafai, K, and Kuzay, T.M, 1995, Effects of boundary conditions on non-Darcian heat transfer through porous media and experimental comparisons, *Numerical Heat Transfer*, Part A, pp.651-664.

[5] Whitaker, S, 1977, Simultaneous heat, mass and momentum transfer in porous media: a theory of drying, *Advances in Heat Transfer*, 13, pp.119-203.

[6] Sozen, M, Vafai, K, 1991, Analysis of oscillating compressible flow through a packed bed ,International Journal of Heat and Fluid Flow, 12, pp.130-136.

[7] Vafai, K, Tien, C.L, 1981, Boundary and inertia effects on flow and heat transfer in porous media, Int. J. Heat Mass Transfer 24 (1981) 195-203.

[8] Vafai, K, Thiyagraja, R, 1987, Analysis of flow and heat transfer at the interface region of a porous medium, Int. J. Heat Mass Transfer, 30, pp.1391-1405.

[9] Lee, D. Y, Vafai, K, 1999, Analytical characterization and conceptual assessment of solid and fluid temperature differentials in porous media, Int. J. Heat Mass Transfer 42 (1999) 423-435.

[10]Kim, S.J, Kim, D, and Lee, D.Y, 2000, On the local thermal equilibrium in micro channel heat sinks, Int. J. Heat Mass Transfer, 43, pp.1735-1748.

[11]Jeng, T.M, Tzeng, S.C, Hung, Y.H, 2006, An analytically study of local thermal equilibrium in porous heat sinks using fin theory, Int. J. Heat Mass Transfer, 49, pp.1907-1914.

[12]Tien, C.Y, Yan, T.Z, 2005, Developing fluid flow and heat transfer in a cannel partially filled with porous medium, Int. J. Heat Mass Transfer, 48, pp.3995-4009.